

**UCC Library and UCC researchers have made this item openly available.  
Please [let us know](#) how this has helped you. Thanks!**

<b>Title</b>	Effects of iron oxides on the anaerobic codigestion performances of the Pennisetum hybrid and kitchen waste
<b>Author(s)</b>	Wo, Defang; Bi, Guican; Li, Lianhua; Kang, Xihui; Kong, Xiaoying; Jiang, Enchen; Xie, Jun
<b>Publication date</b>	2022-08-12
<b>Original citation</b>	Wo, D., Bi, G., Li, L., Kang, X., Kong, X., Jiang, E. and Xie, J. (2022) 'Effects of iron oxides on the anaerobic codigestion performances of the Pennisetum hybrid and kitchen waste', Journal of Environmental Engineering, 148(10), 04022062. doi: 10.1061/(ASCE)EE.1943-7870.0002046
<b>Type of publication</b>	Article (peer-reviewed)
<b>Link to publisher's version</b>	<a href="http://dx.doi.org/10.1061/(ASCE)EE.1943-7870.0002046">http://dx.doi.org/10.1061/(ASCE)EE.1943-7870.0002046</a> Access to the full text of the published version may require a subscription.
<b>Rights</b>	© 2022, ASCE. This material may be downloaded for personal use only. Any other use requires prior permission of the American Society of Civil Engineers. This material may be found at: <a href="https://doi.org/10.1061/(ASCE)EE.1943-7870.0002046">https://doi.org/10.1061/(ASCE)EE.1943-7870.0002046</a>
<b>Item downloaded from</b>	<a href="http://hdl.handle.net/10468/13602">http://hdl.handle.net/10468/13602</a>

Downloaded on 2022-12-08T08:42:21Z



33 co-digestion of the *Pennisetum* hybrid and kitchen waste. The addition of 0.5% Fe<sub>2</sub>O<sub>3</sub>  
34 (with a biogas production of 286.0 ± 61.8 mL/g volatile solid (VS)) and 0.5% Fe<sub>3</sub>O<sub>4</sub>  
35 (with a biogas production of 309.1 ± 22.3 mL/g VS) improved the cumulative biogas  
36 yield by 23.5% and 37.9%, respectively, compared with that of the control group  
37 (with a biogas production of 237.2 ± 30.1 mL/g VS). Further correlation analysis  
38 showed that pH and total ammonia nitrogen were positively correlated with  
39 cumulative biogas yield, whereas bicarbonate alkalinity concentration/volatile  
40 alkalinity concentration and volatile fatty acids were negatively correlated with  
41 cumulative biogas yield. This study provided insights on anaerobic co-digestion of the  
42 *Pennisetum* hybrid and kitchen waste in the presence of iron oxides, which will be  
43 beneficial for further studies in the field of renewable energy production.

44 **Keywords:** Iron oxides; *Pennisetum* hybrid; Kitchen waste; Co-digestion; Biogas

45

## 46 **Introduction**

47 Energy grass is a promising source for biofuel production because of advantages  
48 such as high solar energy conversion efficiency, water use efficiency, high biomass  
49 yield, high adaptability, strong resilience, high cellulose content, and environmental  
50 friendliness (Lewandowskiet al. 2003). Anaerobic digestion (AD), an important  
51 biological waste treatment technology, is widely deployed to convert energy grass into  
52 a renewable energy source for biogas production (Eyl et al. 2020). Types of energy  
53 grass that are feasible feedstocks for AD to produce biogas include *Panicum virgatum*  
54 L. (Massé et al. 2010), *Dactylis glomerata* L. (Rawnsley et al. 2002), *Festuca elata*,  
55 and *Phalaris arundinacea* L. (Seppälä, et al. 2009). *Pennisetum* hybrid  
56 (*Pennsetu-mameicanum* Tift23A × *P. Purpureum* N51), a perennial herbaceous C4  
57 plant, is one of the most developed potential energy crops with the highest dry matter

58 yield of up to 88 MT/year, high leaf-stem ratio, and strong regeneration ability  
59 ([Herrmann et al. 2015](#)).

60 *Pennisetum* hybrid is difficult to degrade during AD resulting in low biogas  
61 production although its carbohydrate content is up to 60% ([Kang et al. 2019](#)). In  
62 addition, problems such as slow start-up, serious crusting, and difficulty in feeding in  
63 and out may arise when digesting energy grass. Currently, strategies for achieving  
64 high degradation efficiency and biogas production from the AD of *Pennisetum* hybrid  
65 include pretreatment and co-digestion with other nitrogen-rich substrates. For  
66 example, compared with an untreated *Pennisetum* hybrid, methane production  
67 increased by 21%, 33%, and 38% after NaOH, liquid hot water, and NaClO<sub>2</sub>  
68 pretreatment, respectively ([Kang et al. 2018](#); [Kang et al. 2020](#); [Kang et al. 2018](#)). The  
69 stable operational organic loading rate increased from 2.0 g volatile solids (VS)/(L·d)  
70 (mono-digestion of *Pennisetum* hybrid) to 4.5–5.0 g VS/(L·d) (co-digestion with cow  
71 manure) in semi-continuous experiments ([Li et al. 2018](#)). These promising results  
72 indicated that the co-digestion of *Pennisetum* hybrid and nitrogen-rich organic waste  
73 synergically increased conversion efficiency and process stability under an optimal  
74 C/N ratio. Another candidate substrate for co-digestion can be kitchen waste as it  
75 contains high organic matter in which AD is prone to acidification. The co-digestion  
76 of 75% food waste and 25% energy grass resulted in 6% more biogas production than  
77 the digestion of food waste only ([Darimani et al. 2020](#)). Therefore, a study speculated  
78 that with an adjustable C/N ratio, the co-digestion of *Pennisetum* hybrid and kitchen  
79 waste could coordinate the digestion rate of the two raw materials, improve the  
80 problems of unbalanced nutrition and long digestion period, and improve digestion  
81 efficiency ([Gao et al. 2021](#)). Moreover, the co-digestion of them may have  
82 applications in multiple functions, including urban pollution control, resource

83 recycling, ecological environment improvement, energy conservation, and emission  
84 reduction, as well as promote the construction of modern ecological and  
85 environmental protection cities (Gao et al. 2017).

86 Iron has been widely used as an additive to improve AD efficiency (Crichton et  
87 al. 2008). Iron-reducing bacteria produced in AD with  $\text{Fe}_2\text{O}_3$  were conducive to the  
88 transformation of complex organic matter into simple organic matter (Zhang et al.  
89 2014).  $\text{Fe}_2\text{O}_3$  nanoparticles ( $\text{nFe}_2\text{O}_3$ ) inhibited methane production from waste  
90 activated sludge (Unsar et al. 2018).  $\text{Fe}_3\text{O}_4$  nanoparticles ( $\text{nFe}_3\text{O}_4$ ) could increase  $\text{CH}_4$   
91 production by directly promoting interspecies electron transfer to facilitate  
92 methanation (Suanon et al. 2016). Studies have shown that  $\text{FeCl}_3$  increased biogas  
93 production by 79.6% compared with that of the control group and altered the  
94 microbial structure (Yu et al. 2015). The biogas production from activated sludge  
95 increased by 29.5% after adding a rusting iron sheet (Zhang et al. 2014). These results  
96 showed that the valence state and particle size of iron have different effects on AD. To  
97 date, studies regarding the effects of iron oxide addition on the anaerobic co-digestion  
98 of *Pennisetum* hybrid and kitchen waste are scarce.

99 Therefore, the innovation of this study is exploring the influences of different  
100 valence state (+3, +8/3), particle size (nanoparticles, non-nanoparticles) of  $\text{Fe}_2\text{O}_3$ ,  
101  $\text{nFe}_2\text{O}_3$ ,  $\text{Fe}_3\text{O}_4$  and  $\text{nFe}_3\text{O}_4$  with different doses (0.5%, 1.0%, and 1.5%, based on the  
102 weight ratio of iron and fresh substrates) on the anaerobic co-digestion of kitchen  
103 waste and *Pennisetum* hybrid under batch-mode mesophilic experiments. The  
104 objectives of this study are to: (1) assess the biogas production potential from the  
105 co-digestion of kitchen waste and *Pennisetum* hybrid, (2) evaluate and compare the  
106 effects of iron oxide addition on the digestion performance of the co-digestion system,  
107 (3) investigate the relationship between biogas production and stability parameters

108 with the addition of iron in different states.

## 109 **Materials and Methods**

### 110 **Materials and inoculum**

111 A *Pennisetum* hybrid used was from the experimental base of our laboratory  
112 (Kang et al. 2018). The *Pennisetum* hybrid was collected cut into pieces of about 2–3  
113 cm. Kitchen waste was collected from the canteen of Guangzhou Institute of Energy  
114 Conversion, Chinese Academy of Sciences (GIEC, CAS), and wiped the bones,  
115 napkins, and garbage bags out. The *Pennisetum* hybrid and kitchen waste were  
116 smashed using a high-speed pulverizer and stored at  $-20\text{ }^{\circ}\text{C}$  before use. The total  
117 solid (TS) content, VS content, and C/N ratio of the *Pennisetum* hybrid were  $23.5\% \pm$   
118  $0.3\%$ ,  $21.0\% \pm 0.6\%$ , and  $31.2 \pm 0.3$ , respectively, whereas those of the kitchen waste  
119 were  $17.7\% \pm 0.5\%$ ,  $16.3\% \pm 0.6\%$ , and  $12.2 \pm 0.1$ . An inoculum was taken from a  
120 mesophilic continuous stirred tank reactor in GIEC, CAS. The TS and VS of the  
121 inoculum were  $1.3\% \pm 0.01\%$  and  $0.7\% \pm 0.03\%$ , respectively. The inoculum was  
122 fully degassed before use for experiments.

### 123 **Iron reagents**

124  $\text{Fe}_2\text{O}_3$ ,  $n\text{Fe}_2\text{O}_3$ ,  $\text{Fe}_3\text{O}_4$ , and  $n\text{Fe}_3\text{O}_4$  were used to explore the effect of iron  
125 reagents on the performance of anaerobic co-digestion of the *Pennisetum* hybrid and  
126 kitchen waste. The iron additives were purchased from Macklin (Casmart, Shanghai,  
127 China), and their purity and particle size are presented in Table 1.

### 128 **Experimental setup and procedures**

129 An experimental device (Fig. S1) used in this study is an automatic biomethane  
130 potential test system II from Bioprocess Control<sup>TM</sup> (Shanghai, China) containing 15

131 reactors with an automatic agitator at the mouth and two catheters at the sealing plug  
132 as the outlet of sample and biogas (Xin et al. 2018); the working volume of the  
133 reactors was 400 mL. The left side was the sampling port, and the right side was  
134 connected with a biogas collection bag. The agitator was set at a stirring frequency of  
135 1-min working and 3-min stopping. The reactors were under the water bath kettle at  
136  $37 \pm 1$  °C. The reactors were flushed with nitrogen to guarantee anaerobic conditions.

137 In the batch experiment, the VS concentration for all experimental groups was  
138 15.0 g VS/L, and the digestion liquid volume was 400 mL. The VS ratio of the  
139 *Pennisetum* hybrid and kitchen waste was 9.5:0.5, which was obtained on a  
140 preliminary experimental basis (Wo et al. 2022). Fe<sub>2</sub>O<sub>3</sub>, nFe<sub>2</sub>O<sub>3</sub>, Fe<sub>3</sub>O<sub>4</sub>, and nFe<sub>3</sub>O<sub>4</sub>  
141 (0.5%, 1.0%, and 1.5%) were added to the reactors. Each group was set in triplicates.  
142 The control group contained the raw materials and inoculum. The experiment lasted  
143 for 21 days.

#### 144 Analytical methods

145 TS and VS were measured per the standard methods (Walter et al. 1998); the pH,  
146 total ammonia nitrogen (TAN) concentration, bicarbonate alkalinity concentration  
147 (IA), and volatile alkalinity concentration (PA) were obtained according to previous  
148 experiments (Jiang et al. 2018; Li et al. 2012; Li et al. 2013). The biogas yield was  
149 collected in the gasbag. The composition of the biogas was determined by gas  
150 chromatography (GC-2014, SHIMADZU, Shanghai, China) with a sample  
151 measurement time of 7 min (Jia et al. 2017). The concentration of volatile fatty acids  
152 (VFAs, mainly including acetic acid and propionic acid) was analyzed using a  
153 high-performance liquid chromatography system (HPLC, e2695, Waters, Shanghai,  
154 China) (Jiang et al. 2018; Cai et al. 2018).

## 155 **Calculation methods**

### 156 **Kinetic model analysis of cumulative biogas yield**

157 For AD in the batch experiment, cumulative biogas yield was estimated using the  
158 modified Gompertz equation Eq. (1):

$$159 \quad y = a \cdot \exp\{-\exp[b \cdot e / a \cdot (c - x) + 1]\} \quad (1)$$

160 where  $x$ ,  $y$  stand for the digestion time and cumulative biogas yield,  $a$ ,  $b$ , and  $c$   
161 stand for the cumulative biogas yield, the maximum production rate, and the digestion  
162 lag time, respectively.  $e$  is the natural logarithm constant, which equals to 2.713. The  
163 coefficient of determination ( $R^2$ ) was used for kinetic model analysis to fit the  
164 methane production curve (Kang et al. 2017; Koyama et al. 2017).

### 165 **Statistical analysis**

166 Charts of daily and cumulative biogas yield as well as the stability parameters  
167 such as pH, IA/PA, TAN, and VFAs were drawn using Origin 9.0; the kinetic model  
168 analysis was performed using the same software; The correlation between biogas  
169 production and stability parameters was investigated by analysis of variance using  
170 SPSS 17.0.

## 171 **Results and discussion**

### 172 **Performances of the anaerobic co-digestion system after Fe<sub>2</sub>O<sub>3</sub> and nFe<sub>2</sub>O<sub>3</sub> added**

#### 173 **Daily and cumulative biogas yields with Fe<sub>2</sub>O<sub>3</sub> and nFe<sub>2</sub>O<sub>3</sub> addition**

174 Biogas production is an important parameter for the AD of organic substrates. As  
175 shown in Fig. 1a, the daily biogas yields of all groups increased, reaching the  
176 maximum yield on day 1 and then decreased gradually following the continuous  
177 decomposition of substrates. The main species of bacteria involved in this process  
178 might be related to hydrogen-producing acetogenic bacteria, hydrogen-consuming



179 acetogenic bacteria, hydrogen-consuming methanogenic bacteria, and acetic  
180 acid-consuming methanogenic bacteria (Zhai et al. 2015; Ye et al. 2008). The highest  
181 daily biogas yield was 53.3 mL/(g VS·d) for the control group. After adding Fe<sub>2</sub>O<sub>3</sub>  
182 with the different concentrations, the daily biogas yield of the 0.5% Fe<sub>2</sub>O<sub>3</sub> group  
183 increased by 4.2% compared with that of the control group. For the groups in which  
184 0.5%, 1.0%, and 1.5% nFe<sub>2</sub>O<sub>3</sub> were added, the maximum daily biogas yields were  
185 44.6 mL/(g VS·d), 51.7 mL/(g VS·d), and 44.3 mL/(g VS·d), respectively, which  
186 were less than those of the control group and the Fe<sub>2</sub>O<sub>3</sub> groups.

187 As shown in Fig. 1b, the cumulative biogas yield of the control group was  
188 237.2 ± 30.1 mL/g VS. The maximum cumulative biogas yield of 286.2 ± 61.8 mL/g  
189 VS was obtained in the 0.5% Fe<sub>2</sub>O<sub>3</sub> group, which increased by 20.6% compared with  
190 that of the control group. The research of Lu et al. (2019) shown that the cumulative  
191 methane yield of swine manure increased by 11.1% after the addition of 75 mmol  
192 Fe<sub>2</sub>O<sub>3</sub> compared with that of the control group. Kato et al. (2013) found that Fe<sub>2</sub>O<sub>3</sub> in  
193 anaerobic digesters can enhance the methane production rate because of direct  
194 interspecies electron transfer. In addition, the cumulative biogas yields of the 1.0%  
195 and 1.5% Fe<sub>2</sub>O<sub>3</sub> groups were 206.0 ± 8.0 mL/g VS and 228.2 ± 5.2 mL/g VS,  
196 respectively. For the nFe<sub>2</sub>O<sub>3</sub> groups, the highest cumulative biogas yield was observed  
197 in the 1.0% nFe<sub>2</sub>O<sub>3</sub> group; its cumulative biogas yield was 219.1 ± 6.3 mL/g VS.  
198 Moreover, the cumulative biogas yields of the 0.5% and 1.5% nFe<sub>2</sub>O<sub>3</sub> groups were  
199 191.2 ± 16.0 mL/g VS and 199.9 ± 2.1 mL/g V, respectively. The cumulative biogas  
200 yield of Fe<sub>2</sub>O<sub>3</sub> groups were higher than nFe<sub>2</sub>O<sub>3</sub> groups, the probable reasons of were  
201 that the nanoparticles were larger and easier to aggregate, which reduced the  
202 effectiveness of some intermediate products that were conducive to microbial  
203 activities (Yang et al. 2013).

## 204 **Stability of the co-digestion system with Fe<sub>2</sub>O<sub>3</sub> and nFe<sub>2</sub>O<sub>3</sub> addition**

205 In AD, the pH, IA/PA, TAN, and VFAs are important indicators of stability  
206 performances (Ma et al. 2020). Fig. 2 shows the effects of Fe<sub>2</sub>O<sub>3</sub> and nFe<sub>2</sub>O<sub>3</sub> addition  
207 on the stability performances of the co-digestion of the *Pennisetum* hybrid and kitchen  
208 waste. The initial pH values (Fig. 2a) of all groups were in the range of 7.98–8.10.  
209 The pH decreased at the early stage of the digestion and reached the minimum value  
210 of about 6.7–7.0 on 2–3 d; this resulted from the rapid production of VFAs under  
211 acidogenesis. The pH then increased in the range of 6.8–7.98. The lowest pH value  
212 was 6.7 in the 1.0% Fe<sub>2</sub>O<sub>3</sub> group on day 3, and the minimum pH values of other  
213 experimental groups were lower than that of the control group; the reason might be  
214 that the additives promoted the decomposition of the substrate. A previous study has  
215 shown that the suitable pH value of an AD system is 6.8–7.2; the pH values in this  
216 study showed that the system ran stably, and no considerable effect on the pH value  
217 was observed after the addition of Fe<sub>2</sub>O<sub>3</sub> and nFe<sub>2</sub>O<sub>3</sub> (Ward et al. 2008).

218 The IA/PA, similar to the ratio of VFAs to alkalinity, can act as the index of  
219 digester stability (Ripley et al. 1986). The IA/PA value less than 1 implies the stable  
220 state of the digestion system (Ferrer et al. 2010; Martín et al. 2013). As shown in Fig.  
221 2b, in the early stage of digestion reaction (2–5 d), the IA/PA values in all groups  
222 were more than 1.0; the addition of Fe<sub>2</sub>O<sub>3</sub> and nFe<sub>2</sub>O<sub>3</sub> led to higher values, indicating  
223 the unstable digestion system at this period. After day 5, the system gradually returned  
224 to a steady state. The fast increase in IA/PA in the early stage was related to the  
225 increased VFAs concentration with the continuous decomposition of the substrates;  
226 these VFAs were gradually consumed by methane-producing microorganisms in the  
227 methanogenesis stage to produce CH<sub>4</sub> and CO<sub>2</sub> (Noonari et al. 2018). The digestion  
228 systems of the nFe<sub>2</sub>O<sub>3</sub> groups were more stable than those of the Fe<sub>2</sub>O<sub>3</sub> groups; this

229 might be because the addition of  $n\text{Fe}_2\text{O}_3$  helped microorganisms better adapt to the  
230 digestion environment and promoted the effective utilization of intermediate products  
231 such as VFAs.

232 The TAN concentrations (Fig. 2c) of all groups were ranged in 285–640 mg/L  
233 and were less than the inhibition threshold (Chen et al. 2008). The addition of  $\text{Fe}_2\text{O}_3$   
234 and  $n\text{Fe}_2\text{O}_3$  slightly increased the volatility of the co-digestion system because of  
235 substrate decomposition.

236 AD is divided into four stages: hydrolysis, acidogenesis, acetogenesis, and  
237 methanogenesis (Madsen et al. 2011). At the beginning of digestion, the concentration  
238 of VFAs (Fig. 2d) increased along with the degradation of the raw materials. The  
239 VFAs concentration (0–1666.0 mg/L) of all groups increased to the maximum values  
240 in 3–4 d, and then constantly decreased; these were in accordance with the variations  
241 in the pH value and IA/PA ratio. During the entire digestion, the VFAs concentrations  
242 in all groups were below the inhibition threshold (Strau et al. 2012; Xiao et al. 2013).  
243 In the later stage of the digestion, VFAs concentration was below the test  
244 concentration because of the complete consumption of the substrates by  
245 microorganisms.

246 From the discussion above, compared with the control group, the  $\text{Fe}_2\text{O}_3$  and  
247  $n\text{Fe}_2\text{O}_3$  groups had insignificant effects on stability parameters (pH, IA/PA, TAN, and  
248 VFAs) of anaerobic co-digestion of the *Pennisetum* hybrid and kitchen waste. As the  
249 system itself was not under extreme stress conditions, the regulating effect was not  
250 considerable. Similarly, the VFAs and pH did not change significantly in the AD of  
251 cattle manure (Farghali et al. 2019).

252 **Performances of the anaerobic co-digestion system after  $\text{Fe}_3\text{O}_4$  and  $n\text{Fe}_3\text{O}_4$  added**

253 **Daily and cumulative biogas yields with  $\text{Fe}_3\text{O}_4$  and  $n\text{Fe}_3\text{O}_4$  addition**

254 Similar to trends of the  $\text{Fe}_2\text{O}_3$  and  $\text{nFe}_2\text{O}_3$  group yields, and the maximum daily  
255 biogas yields of all groups of  $\text{Fe}_3\text{O}_4$  and  $\text{nFe}_3\text{O}_4$  (Fig. 3a) were ranged in 41.0–60.6  
256  $\text{mL}/(\text{g VS}\cdot\text{d})$ . The highest value of the daily biogas yield was 60.6  $\text{mL}/(\text{g VS}\cdot\text{d})$   
257 observed in the 0.5%  $\text{Fe}_3\text{O}_4$  group and increased by 13.6% compared with that of the  
258 control group. The daily biogas yields of the  $\text{Fe}_3\text{O}_4$  and  $\text{nFe}_3\text{O}_4$  experimental groups  
259 were lower than that of the control group except for the 0.5%  $\text{Fe}_3\text{O}_4$  group.

260 As shown in Fig. 3b, the cumulative biogas yields of the  $\text{Fe}_3\text{O}_4$  and  $\text{nFe}_3\text{O}_4$   
261 groups were ranged in  $204.2 \pm 18.4$ – $309.1 \pm 22.3$   $\text{mL}/\text{g VS}$  and  $226.3 \pm 5.8$ – $236.4 \pm$   
262  $11.2$   $\text{mL}/\text{g VS}$ , respectively. The maximum value of cumulative biogas yield was  
263 observed in the 0.5%  $\text{Fe}_3\text{O}_4$  group ( $309.1 \pm 22.3$   $\text{mL}/\text{g VS}$ ). The cumulative biogas  
264 yields of other groups were  $222.4 \pm 44.8$   $\text{mL}/\text{g VS}$  (1.0%  $\text{Fe}_3\text{O}_4$ ),  $204.2 \pm 28.4$   $\text{mL}/\text{g}$   
265  $\text{VS}$  (1.5%  $\text{Fe}_3\text{O}_4$ ),  $226.4 \pm 2.4$   $\text{mL}/\text{g VS}$  (0.5%  $\text{nFe}_3\text{O}_4$ ),  $236.4 \pm 11.2$   $\text{mL}/\text{g VS}$  (1.0%  
266  $\text{nFe}_3\text{O}_4$ ), and  $226.3 \pm 5.8$   $\text{mL}/\text{g VS}$  (1.5%  $\text{nFe}_3\text{O}_4$ ), which were decreased compared  
267 with that of the control group.

### 268 **Stability of the co-digestion system with $\text{Fe}_3\text{O}_4$ and $\text{nFe}_3\text{O}_4$ addition**

269 The effects of stability performances of  $\text{Fe}_3\text{O}_4$  and  $\text{nFe}_3\text{O}_4$  on the co-digestion of  
270 the *Pennisetum* hybrid and kitchen waste are presented in Fig. 4.

271 The pH was almost similar between the  $\text{Fe}_2\text{O}_3$  and  $\text{nFe}_2\text{O}_3$  groups, which first  
272 decreased and then increased until ranged in 6.9–7.9 from the initial values of 7.7–8.1  
273 (Fig. 4a). The lowest pH value was 6.86 for the 1.5%  $\text{nFe}_3\text{O}_4$  group on day 3. The pH  
274 values stayed in a suitable range during the whole process. In the early stage of  
275 digestion reaction, the IA/PA values were increased and were more than 1 on 2–3 d,  
276 and then the systems gradually returned to a steady state ranging in 0.1–0.9, which  
277 was related to the changes in VFA concentration (Fig. 4b). The maximum TAN  
278 concentrations of the  $\text{Fe}_3\text{O}_4$  and  $\text{nFe}_3\text{O}_4$  groups were 435  $\text{mg}/\text{L}$  (0.5%  $\text{Fe}_3\text{O}_4$ ), 430

279 mg/L (1.0% Fe<sub>3</sub>O<sub>4</sub>), 410 mg/L (1.5% Fe<sub>3</sub>O<sub>4</sub>), 410 mg/L (0.5% nFe<sub>3</sub>O<sub>4</sub>), 390 mg/L (1.0%  
280 nFe<sub>3</sub>O<sub>4</sub>), and 410 mg/L (1.5% nFe<sub>3</sub>O<sub>4</sub>) (Fig. 4c). No considerable change was  
281 observed in the aforementioned groups compared with the control group (308–408  
282 mg/L) and the TAN concentrations of the experimental groups were less than the  
283 inhibition threshold (Chen et al. 2008). The VFAs concentration ranged in 0–1568.6  
284 mg/L during the first 21 days and did not exceed the inhibition value (Strau et al. 2012;  
285 Xiao et al. 2013).

286 To sum up, the Fe<sub>3</sub>O<sub>4</sub> groups showed no significant effects on the stability  
287 parameters after the addition of Fe<sub>3</sub>O<sub>4</sub> and nFe<sub>3</sub>O<sub>4</sub> with different concentrations  
288 compared with the control group.

### 289 **Kinetic dynamic parameters of the co-digestion system after the addition of** 290 **different iron reagents**

291 The kinetic analysis of the cumulative biogas yield after the addition of different  
292 iron reagents is shown in Fig. 5 and Table 2. The modified Gompertz equation Eq. (1)  
293 presented very high coefficients for most of the groups of Fe<sub>2</sub>O<sub>3</sub>, nFe<sub>2</sub>O<sub>3</sub>, Fe<sub>3</sub>O<sub>4</sub>, and  
294 nFe<sub>3</sub>O<sub>4</sub> as R<sup>2</sup> was greater than 0.900. The *a* of the control group was 242.7 ± 4.6 mL/g  
295 VS, whereas the *b* was 34.9 ± 2.4 mL/g VS. The best group for maximum biogas  
296 production was the system with the addition of 0.5% Fe<sub>3</sub>O<sub>4</sub> and its value was 316.7 ±  
297 6.07 mL/g VS, which increased by 30.5% compared with that of the control group.  
298 The *b* is an indicator of the biodegradability and digestion efficiency of substrates  
299 (Donoso et al. 2010). The higher the value, the faster the degradation rate of organic  
300 matter and the biogas production rate. The maximum production rate of 42.4 ± 2.7  
301 mL/(g VS·d) was obtained for the system with 0.5% Fe<sub>3</sub>O<sub>4</sub>, which increased by 21.2%  
302 compared with that of the control group. Based on the *c* value, the lag times of all  
303 groups were less than 1.

## 304 **Correlation analysis between the biogas production and stability parameters**

305 The correlation analysis was performed via Spearman's correlation coefficient  
306 ( $r_s$ ). As presented in Fig. 6, pH (moderate correlation) and TAN (weak or moderate  
307 correlation) were positively correlated with the cumulative biogas yield, whereas  
308 IA/PA (moderate or strong correlation) and VFAs (strong correlation) were negatively  
309 correlated with the cumulative biogas yield. In Fig. 6,  $|r_s| = 0.6-1.0$ : Dark-grey  
310 shading strong correlation;  $|r_s| = 0.4-0.6$ : light-grey shading moderate correlation;  
311  $|r_s|=0-0.4$ : no shading weak or no correlation. \*: The correlation was significant at a  
312 confidence interval of 0.05; \*\*: The correlation was significant at a confidence  
313 interval of 0.01. Negative values indicate that the two factors are negatively correlated,  
314 and positive values indicate that the two factors are positively correlated.

315 For the cumulative biogas yield and IA/PA, the  $r_s$  of the  $Fe_3O_4$  and  $nFe_3O_4$  groups  
316 were stronger than that of the  $Fe_2O_3$  and  $nFe_2O_3$  groups, indicating that biogas  
317 production in the  $Fe_3O_4$  and  $nFe_3O_4$  groups was more likely to be affected by system  
318 stability. On the contrary, for the cumulative biogas yield and VFAs, the  $r_s$  of the  
319  $Fe_2O_3$  and  $nFe_2O_3$  groups were stronger than that of the  $Fe_3O_4$  and  $nFe_3O_4$  groups,  
320 indicating that the biogas production in the  $Fe_2O_3$  and  $nFe_2O_3$  groups were more  
321 sensitive to VFA changes.

## 322 **Comparison of the co-digestion performance of the kitchen waste and** 323 ***Pennisetum* hybrid in different conditions**

324 The experimental results showed that the additives with different valence states  
325 and particle sizes exhibited different effects on the anaerobic co-digestion of the  
326 *Pennisetum* hybrid and kitchen waste (Fig. 6).

327 A significant difference in the cumulative biogas yields of the  $Fe_2O_3$  and  $Fe_3O_4$

328 groups was observed, and the concentration of 0.5% of them showed a promising  
329 effect. The potential mechanism of  $\text{Fe}_2\text{O}_3$  might be attributed to 1) alter microbial  
330 communities as the trace element; 2) improve extracellular polymer substances  
331 characteristics through the concentrations of soluble proteins and polysaccharides; 3)  
332 enhance the direct interspecies electron transfer (DIET) between acetogens and  
333 methanogens (Cai et al. 2016; Ye et al. 2018; Wang et al. 2018). For the  $\text{Fe}_3\text{O}_4$ , the  
334 reason of increasing the biogas yield maybe that it facilitates the DIET, and alter the  
335 enzymes and microbial community (Zhou et al. 2021).

336 In general, the material with large specific surface area had the larger contact  
337 area with the raw material, and the promotion effect was better in the appropriate  
338 concentration range (Kumar et al. 2021). On the other hand, the force between small  
339 size particles was larger and easier to aggregate; as a result, the effective reacting  
340 concentration or some intermediate products that were conducive to microbial  
341 activities were reduced (Yang et al. 2013). Overall, the addition of the two additives  
342 had an inhibitory effect on the biogas production capacity of the digestion system  
343 when the concentration was more than 1.0% (Suanon et al. 2017). And the stability  
344 was better in the  $\text{Fe}_3\text{O}_4$  group than in the  $\text{nFe}_3\text{O}_4$  group, especially after the addition  
345 of 1.5%  $\text{Fe}_3\text{O}_4$ . This could be because the concentrations such as 1.0% and 1.5% were  
346 beyond the critical value and suitable range for system microorganisms and  
347 intermediates. The reason might be the finest particle size of  $\text{nFe}_3\text{O}_4$  was easy to  
348 aggregate, resulting in insufficient contact with the substrates. Moreover, when more  
349 concentration of  $\text{nFe}_3\text{O}_4$  was added, a higher degree of aggregation state was observed,  
350 which might also affect the decomposition and utilization of substrates by  
351 microorganisms in the digestion (Ajayi et al. 2021).

352 By comparing Fig. 2 and Fig. 4, we concluded that the system stability of the

353 Fe<sub>3</sub>O<sub>4</sub> and nFe<sub>3</sub>O<sub>4</sub> groups was better than that of the Fe<sub>2</sub>O<sub>3</sub> and nFe<sub>2</sub>O<sub>3</sub> groups  
354 according to the fluctuations of IA/PA values. As a whole, the lowest pH values in the  
355 Fe<sub>3</sub>O<sub>4</sub> and nFe<sub>3</sub>O<sub>4</sub> groups were significantly higher than those in the Fe<sub>2</sub>O<sub>3</sub> and  
356 nFe<sub>2</sub>O<sub>3</sub> groups, indicating that Fe<sub>3</sub>O<sub>4</sub> and nFe<sub>3</sub>O<sub>4</sub> had more promotional effects on the  
357 digestion environment and preventing acidification via enhancing the effective  
358 utilization of VFAs by microorganisms.

## 359 **Conclusions**

360 The addition of iron oxides exhibited different effects on the anaerobic  
361 co-digestion of the *Pennisetum* hybrid and kitchen waste. The detailed analysis  
362 showed that the biogas yields increased after adding 0.5% Fe<sub>2</sub>O<sub>3</sub> and 0.5% Fe<sub>3</sub>O<sub>4</sub> into  
363 the co-digestion system. Compared with the control group yields, the cumulative  
364 biogas yield was  $286.0 \pm 61.8$  mL/g VS for the 0.5% Fe<sub>2</sub>O<sub>3</sub> group and  $309.1 \pm 22.3$   
365 mL/g VS for the 0.5% of Fe<sub>3</sub>O<sub>4</sub> group, which increased by 23.5% and 27.3%,  
366 respectively. This study confirmed that iron oxides with different particle sizes and  
367 valence states had different effects on biogas production and stability parameters,  
368 providing fundamental information on the anaerobic co-digestion of the kitchen waste  
369 and *Pennisetum* hybrid.

## 370 **Data Availability Statement**

371 All data, models, and code generated or used during the study appear in the  
372 submitted article.

## 373 **Acknowledgements**

374 This work was supported by the National Natural Science Foundation of China  
375 (21978289); Guangdong Science and Technology Planning Project of Guangdong



376 (2017B020238005); Key Research and Development Program of Jiangxi Province

377 (20171ACG70020).

378

379

380

381

382

383

384

385

386

387

388

389

390

391

392

393

394

395

396

397 **Reference**

- 398 Ajayi, B., A. A., Rahman, S.. 2021. “Efficacy of magnetite (Fe<sub>3</sub>O<sub>4</sub>) nanoparticles for enhancing  
399 solid-state anaerobic co-digestion: Focus on reactor performance and retention time.”  
400 *Bioresour. Technol.* 324(1):124670. <https://doi.org/10.1016/j.biortech.2021.124670>
- 401 Cai, Y., Wang, J., Zhao, Y., Zhao, X., Zheng, Z., Wen, B., Wang, X.. 2018. “A new perspective of  
402 using sequential extraction: To predict the deficiency of trace elements during anaerobic  
403 digestion.” *Water. Res.* S0043135418303415. <https://doi.org/10.1016/j.watres.2018.04.047>
- Cai, Y., Zhao, X. Zhao, Y., Wang, H., Yuan, X., Zhu, W., Cui, Z., Wang, X.. 2017. “Optimization  
of Fe<sup>2+</sup> supplement in anaerobic digestion accounting for the Fe-bioavailability.” *Bioresour.  
Technol.* 250, 163-170. <https://doi.org/10.1016/j.biortech.2017.07.151>
- 404 Chen, Y., Cheng, J., Creamer, K.. 2008. “Inhibition of anaerobic digestion process: A review.”  
405 *Bioresour. Technol.* 99(10) 4044-4064. <https://doi.org/10.1016/j.biortech.2007.01.057>
- 406 Crichton, R. R.. 2008. “Iron: Essential for Almost All Life.” *J. Biol. Inorg. Chem.* 211-240.  
407 <https://doi.org/10.1016/B978-044452740-0.50013-2>
- 408 Darimani, H. S., Pant, D. C.. 2020. “Biogas Production from Co-Digestion of Grass with Food  
409 Waste.” *JAgr. Chem. Environment.* 9(1):10. <https://doi.org/10.4236/jacen.2020.91003>
- 410 Donoso, B., A., Pérez-Elvira S. I., Fdz-Polanco, F.. 2010. “Application of simplified models for  
411 anaerobic biodegradability tests. Evaluation of pre-treatment processes.” *Cheml. Eng. J.*  
412 160(2):607-614. <https://doi.org/10.1016/j.cej.2010.03.082>
- 413 Eyl, A., Ht, B., Yc, C., Kn, C., Jz, D., B, Y.W.. 2020. “Methanogenic pathway and microbial  
414 succession during start-up and stabilization of thermophilic food waste anaerobic digestion  
415 with biochar.” *Bioresour. Technol.* 314. <https://doi.org/10.1016/j.biortech.2020.123751>
- 416 Farghali, M., Andriamanohiarisoamanana, F. J., Ahmed, M. M., Kotb, S., Yamashiro, T., Iwasaki,  
417 Umetsu, K.. 2019. “Impacts of iron oxide and titanium dioxide nanoparticles on biogas  
418 production: Hydrogen sulfide mitigation, process stability, and prospective challenges.” *J.  
419 Environ. Manage.* 240(JUN.15):160-167. <https://doi.org/10.1016/j.jenvman.2019.03.089>
- 420 Ferrer, I., Vázquez, F., Font, X.. 2010. “Long term operation of a thermophilic anaerobic reactor:  
421 Process stability and efficiency at decreasing sludge retention time.” *Bioresour. Technol.*  
422 101(9), 2972-2980. <https://doi.org/10.1016/j.biortech.2009.12.006>

423 Gao, M., Yang, M., Ma, X., Xie, D., Wang, Q.. 2021. "Effect of co-digestion of tylosin  
424 fermentation dreg and food waste on anaerobic digestion performance." *Bioresour. Technol.*  
425 325(36):124693. <https://doi.org/10.1016/j.biortech.2021.124693>

426 Gao, P., Gu, C., Wei, X., Li, X., Chen, H., Jia, H., Liu, Z., Xue, G., Ma, C.. 2017. "The role of  
427 zero valent iron on the fate of tetracycline resistance genes and class 1 integrons during  
428 thermophilic anaerobic co-digestion of waste sludge and kitchen waste." *Water. Res.*  
429 111:92-99. <https://doi.org/10.1016/j.watres.2016.12.047>

430 Herrmann, C., Prochnow, A., Heiermann, M., Idler, C.. 2015. "Biomass from landscape  
431 management of grassland used for biogas production: effects of harvest date and silage  
432 additives on feedstock quality and methane yield." *Grass. Forage. Sci.* 69(4):549-566.  
433 <https://doi.org/10.1111/gfs.12086>

434 Jia, T., Wang, Z., Shan, H., Liu, Y., Lei, G.. 2017. "Effect of nanoscale zero-valent iron on sludge  
435 anaerobic digestion." *Resour. Conserv. Recy.* 127:190-195.  
436 <https://doi.org/10.1016/j.resconrec.2017.09.007>

437 Jiang, J., Li, L., Cui, M., Zhang, F., Liu, Y., Liu, Y., Long, J., Guo, Y.. 2018. "Anaerobic digestion  
438 of kitchen waste: the effects of source, concentration, and temperature." *Biochem. Eng. J.* 135,  
439 91-97. <https://doi.org/10.1016/j.bej.2018.04.004>

440 Kang, X., Sun, Y., Li, L., Kong, X., Yuan, Z.. 2018. "Improving methane production from  
441 anaerobic digestion of *Pennisetum* Hybrid by alkaline pretreatment." *Bioresour. Technol.* 255,  
442 205-212. <https://doi.org/10.1016/j.biortech.2017.12.001>

443 Kang, X., Zhang, Y., Song, B., Sun, Y., Li, L., He, Y., Kong, X., Luo, X., Yuan, Z.. 2019. "The  
444 effect of mechanical pretreatment on the anaerobic digestion of Hybrid *Pennisetum*." *Fuel.*  
445 252(15):469-474. <https://doi.org/10.1016/j.fuel.2019.04.134>

446 Kang, X., Sun, Y., Li, L., Kong, X., Yuan, Z.. 2018. "Improving methane production from  
447 anaerobic digestion of *Pennisetum* Hybrid by alkaline pretreatment." *Bioresour. Technol.*  
448 <https://doi.org/10.1016/j.biortech.2017.12.001>

449 Kang, X., Zhang, Y., Lin, R., Li, L., Zhen, F., Kong, X., Sun, Y., Yuan, Z.. 2020. "Optimization of  
450 liquid hot water pretreatment on Hybrid *Pennisetum* anaerobic digestion and its effect on  
451 energy efficiency." *Energ. ConversManage.* 210.

452 <https://doi.org/10.1016/j.enconman.2020.112718>

453 Kang, X., Zhang, Y., Li, L., Sun, Y., Kong, X.. 2019. “Enhanced methane production from  
454 anaerobic digestion of hybrid *Pennisetum* by selectively removing lignin with sodium  
455 chlorite.” *Bioresour. Technol.* <https://doi.org/10.1016/j.biortech.2019.122289>

456 Kato, S., Hashimoto, K., Watanabe, K.. 2013. “Iron-oxide minerals affect extracellular  
457 electron-transfer paths of geobacter spp.” *Microbes. Environ.* 28 (1), 141-148.  
458 <https://doi.org/10.1264/jsme2.ME12161>

459 Koyama, M., Yamamoto, S., Ishikawa, K., Ban, S., Toda, T.. 2017. “Inhibition of anaerobic  
460 digestion by dissolved lignin derived from alkaline pre-treatment of an aquatic macrophyte.”  
461 *Chem. Eng. J.* 311, 55-62. <https://doi.org/10.1016/j.cej.2016.11.076>

462 Kumar, S. S., Ghosh, P., Kataria, N., Kumar, D., Thakur, S.. 2021. “The Role of Conductive  
463 Nanoparticles in Anaerobic Digestion: Mechanism, Current Status and Future Perspectives.”  
464 *Chemosphere.* <https://doi.org/10.1016/j.chemosphere.2021.130601>

465 Lewandowski, I., Scurlock, J. M. O., Lindvall, E., Christou, M.. 2003. “The development and  
466 current status of perennial rhizomatous grasses as energy crops in the US and Europe.”  
467 *Biomass Bioenerg.* 25(4):335-361. [https://doi.org/10.1016/S0961-9534\(03\)00030-8](https://doi.org/10.1016/S0961-9534(03)00030-8)

468 Li, L., Kong, X., Yang, F., Li, D., Yuan, Z., Sun, Y.. 2012. “Biotechnology. Biogas Production  
469 Potential and Kinetics of Microwave and Conventional Thermal Pretreatment of Grass.” *Appl.*  
470 *Biochem. Biotechnol.* 166(5), 1183-1191. <https://doi.org/10.1007/s12010-011-9503-9>

471 Li, L., Li, Y., Sun, Y., Yuan, Z., Lv, P., Kang, X., Zhang, Y., Yang, G.. 2018. “Influence of the  
472 Feedstock Ratio and Organic Loading Rate on the Co-digestion Performance of *Pennisetum*  
473 hybrid and Cow Manure.” *Energy. Fuels.* 32(4):5171-5180.  
474 <https://doi.org/10.1021/acs.energyfuels.8b00015>

475 Li, Y., Zhang, R., Chen, C., Liu, G., He, Y., Liu, X.. 2013. “Biogas production from co-digestion  
476 of corn stover and chicken manure under anaerobic wet, hemi-solid, and solid state  
477 conditions.” *Bioresour. Technol.* 149(4), 406-412.  
478 <https://doi.org/10.1016/j.biortech.2013.09.091>

479 Lu, T., Zhang, J., Wei, Y., Shen, P.. 2019. “Effects of ferric oxide on the microbial community and  
480 functioning during anaerobic digestion of swine manure.” *Bioresour. Technol.* 287:121393.

481 <https://doi.org/10.1016/j.biortech.2019.121393>

482 Ma, X., Yu, M., Song, N.a., Xu, B., Gao, M., Wu, C., Wang, Q.. 2020. "Effect of ethanol  
483 pre-fermentation on organic load rate and stability of semi-continuous anaerobic digestion of  
484 food waste." *Bioresour. Technol.* 299, 122587. <https://doi.org/10.1016/j.biortech.2019.122587>

485 Madsen, M., Holm-Nielsen, J. B., Esbensen, K. H.. 2011. "Monitoring of anaerobic digestion  
486 processes: A review perspective." *Renew Sust Energy Rev.* 15(6):3141-3155.  
487 <https://doi.org/10.1016/j.rser.2011.04.026>

488 Massé, D., Gilbert, Y., Savoie, P., Bélanger, G., Parent, G., Babineau, D.. 2010. "Methane yield  
489 from switchgrass harvested at different stages of development in Eastern Canada." *Bioresour.*  
490 *Technol.* 101(24):9536. <https://doi.org/10.1016/j.biortech.2010.07.018>

491 Martín, G. L., Font, X., Vicent, T.. 2013. "Alkalinity ratios to identify process imbalances in  
492 anaerobic digesters treating source-sorted organic fraction of municipal wastes." *Biochem.*  
493 *Eng. J.* 76, 1-5. <https://doi.org/10.1016/j.bej.2013.03.016>

494 Zhai, N., Zhang, T., Z., Yin, D., Yang, G., W, X., W., Ren, G., Feng, Y.. 2015. "Effect of initial pH  
495 on anaerobic co-digestion of kitchen waste and cow manure." *Waste. Manage.* 38(1),  
496 126-131. <https://doi.org/10.1016/j.wasman.2014.12.027>

497 Noonari, A., Mahar, R., Sahito, A., Brohi, K.. 2018. "Anaerobic Co-digestion of canola straw and  
498 banana plant wastes with buffffalo dung: effffect of Fe<sub>3</sub>O<sub>4</sub> nanoparticles on methane yield."  
499 *Renew. Energy.* <https://doi.org/10.1016/j.renene.2018.10.113>

500 Rawnsley, R. P., Donaghy, D. J., Fulkerson, W. J., Lane, P. A.. 2002. "Changes in the physiology  
501 and feed quality of cocksfoot (*Dactylis glomerata* L.) during regrowth." *Grass. Forage. Sci.*  
502 57(3):203-211. <https://doi.org/10.1046/j.1365-2494.2002.00318.x>

503 Ripley, L.E., Boyle, W.C., Converse, J.C. 1986. "Improved alkalimetric monitoring for anaerobic  
504 digestion of high strength wastes." *J. Water. Poll. Control. Fed.* 58, 406-411.

505 Seppälä, M., Paavola, T., Lehtomäki, A., Rintala, J.. 2009. "Biogas production from boreal  
506 herbaceous grasses-specific methane yield and methane yield per hectare." *Bioresour.*  
507 *Technol.* 100(12):2952-2958. <https://doi.org/10.1016/j.biortech.2009.01.044>

508 Strau, C., Vetter, A., Felde, A. V.. 2016. "Biogas Production and Energy Crops." *Biodiesel.* 35(02):  
509 72-76. (in Chinese) [https://doi.org/10.1007/978-1-4614-5820-3\\_313](https://doi.org/10.1007/978-1-4614-5820-3_313)

510 Suanon, F., Sun, Q., Mama, D., Li, J., Dimon, B., Yu, C.. 2016. "Effect of nanoscale zero-valent  
511 iron and magnetite (Fe<sub>3</sub>O<sub>4</sub>) on the fate of metals during anaerobic digestion of sludge." *Water*  
512 *Res.* 88:897-903. <https://doi.org/10.1016/j.watres.2015.11.014>

513 Suanon, F., Qian, S., Li, M., Xiang, C., Zhang, Y., Yan, Y., Yu, C.. 2017. "Application of nanoscale  
514 zero valent iron and iron powder during sludge anaerobic digestion: Impact on methane yield  
515 and pharmaceutical and personal care products degradation." *J. Hazard. Mater.* 321, 47-53.  
516 <https://doi.org/10.1016/j.jhazmat.2016.08.076>

517 Unsar, E. K., Perendeci, N. A.. 2018. "What kind of effects do Fe<sub>2</sub>O<sub>3</sub> and Al<sub>2</sub>O<sub>3</sub> nanoparticles have  
518 on anaerobic digestion, inhibition or enhancement?" *Chemosphere.* 211(NOV.):726-735.  
519 <https://doi.org/10.1016/j.chemosphere.2018.08.014>

520 Walter, W.G.. 1998. "APHA Standard Methods for the Examination of Water and Wastewater."  
521 *American Journal of Public Health & the Nations Health.* 56(3)387.  
522 <https://doi.org/10.2105/AJPH.56.4.684-a>

523 Wang, M., Zhao, Z., Niu, J., Zhang, Y.. 2018. "Potential of crystalline and amorphous ferric oxides for  
524 biostimulation of anaerobic digestion." *ACS. Sustain. Chem. Eng.* 7 (1), 697-708.  
525 <https://doi.org/10.1021/acssuschemeng.8b04267>

526 Ward, A. J., Hobbs, P. J., Holliman, P. J., Jones, D. L.. 2008. "Optimisation of the anaerobic  
527 digestion of agricultural resources." *Bioresour. Technol.* 99(17):7928-7940.  
528 <https://doi.org/10.1016/j.biortech.2008.02.044>

529 Wo, D., Bi, G., Li, L., Kong, X., Jiang, E., Xie, J.. 2022. "Iron-fortified anaerobic co-digestion  
530 performance of kitchen waste and *Pennisetum* hybrid." *BioEnerg. Res.*  
531 <https://doi.org/10.1007/s12155-022-10426-0>

532 Xiao, K., Guo, C., Zhou, Y., Maspolim, Y., Wang, J., Ng, W.. 2013. "Acetic acid inhibition on  
533 methanogens in a two-phase anaerobic process." *Biochem. Eng. J.* 75(Complete):1-7.  
534 <https://doi.org/10.1016/j.bej.2013.03.011>

535 Xin, K., Yu, S., Shuang, X., Wen, F., Liu, J., Li, H. 2017. "Effect of Fe<sup>0</sup>, addition on volatile fatty  
536 acids evolution on anaerobic digestion at high organic loading rates." *Waste. Manage.*  
537 71(JAN.), 719-727. <https://doi.org/10.1016/j.wasman.2017.03.019>

538 Yang, Y., Guo, J., Hu, Z.. 2013. "Impact of nano zero valent iron (NZVI) on methanogenic activity

539 and population dynamics in anaerobic digestion.” *Water. Res.* 47(17)6790.  
540 <https://doi.org/10.1016/j.watres.2013.09.012>

541 Ye, C., Cheng, J., Creamer, K.. 2008. “Inhibition of anaerobic digestion process: a review.”  
542 *Bioresour. Technol.* 99(10), 4044-4064. <https://doi.org/10.1016/j.biortech.2007.01.057>

543 Yu, B., Lou, Z., Zhang, D., Shan, A., Zhang, K.. 2015. “Variations of organic matters and  
544 microbial community in thermophilic anaerobic digestion of waste activated sludge with the  
545 addition of ferric salts.” *Bioresour. Technol.* 179:291-298.  
546 <https://doi.org/10.1016/j.biortech.2014.12.011>

547 Ye, J., Hu, A., Ren, G., Chen, M., Tang, J., Zhang, P., Zhou, S., He, Z.. 2018. “Enhancing sludge  
548 methanogenesis with improved redox activity of extracellular polymeric substances by  
549 hematite in red mud.” *Water. Res.* 134, 54-62. <https://doi.org/10.1016/j.watres.2018.01.062>

550 Zhang, Y., Feng, Y., Yu, Q., Xu, Z., Quan, X.. 2014. “Enhanced high-solids anaerobic digestion of  
551 waste activated sludge by the addition of scrap iron.” *Bioresour. Technol.* 159(5):297-304.  
552 <https://doi.org/10.1016/j.biortech.2014.02.114>

Zhou, J., Zhang, H., Liu, J., Gong, L., Yang, X., Zuo, T., Wang, J., X., Jia, Q., Wang, L.. 2021.  
“Effects of Fe<sub>3</sub>O<sub>4</sub> nanoparticles on anaerobic digestion enzymes and microbial community of  
sludge.” *Environ. Technol.* 9, 1-26. <https://doi.org/10.1080/09593330.2021.1963324>

**Table 1.** Characteristics of four iron oxides.

Parameter	Unit	Fe <sub>2</sub> O <sub>3</sub>	nFe <sub>2</sub> O <sub>3</sub>	Fe <sub>3</sub> O <sub>4</sub>	nFe <sub>3</sub> O <sub>4</sub>
Purity	%	69.5–70.1	99.5	99.0	99.5
Particle size	μm/nm	5 μm	30 nm	2 μm	20 nm

**Table 2.** Kinetic analysis of co-digestion at different conditions.

Group	Dosage	<i>a</i> (mL/g VS)	<i>b</i> (mL/g VS·d)	<i>c</i> (d)	R <sup>2</sup>
Control	-	242.7 ± 4.6	34.9 ± 2.4	0.2 ± 0.2	0.988
Fe <sub>2</sub> O <sub>3</sub>	0.5%	287.8 ± 4.7	35.2 ± 1.8	0.1 ± 0.2	0.992
	1.0%	210.8 ± 4.5	29.4 ± 2.2	0.1 ± 0.3	0.983
	1.5%	233.8 ± 5.0	32.0 ± 2.3	0.1 ± 0.3	0.985
nFe <sub>2</sub> O <sub>3</sub>	0.5%	195.4 ± 4.1	25.8 ± 1.8	0.0 ± 0.3	0.986
	1.0%	224.1 ± 4.5	30.1 ± 2.0	0.0 ± 0.3	0.987
	1.5%	204.8 ± 4.1	27.5 ± 1.9	0.1 ± 0.3	0.987
Fe <sub>3</sub> O <sub>4</sub>	0.5%	316.7 ± 6.0	42.4 ± 2.7	0.3 ± 0.2	0.989
	1.0%	213.7 ± 4.6	28.9 ± 2.1	0.1 ± 0.3	0.985
	1.5%	210.0 ± 4.5	29.4 ± 2.2	0.3 ± 0.3	0.985
nFe <sub>3</sub> O <sub>4</sub>	0.5%	233.7 ± 5.7	26.9 ± 1.9	0.4 ± 0.3	0.986
	1.0%	245.0 ± 5.8	27.6 ± 1.8	0.3 ± 0.3	0.987
	1.5%	233.8 ± 5.6	26.7 ± 1.8	0.4 ± 0.3	0.987



555 **Figure Caption List:**

556 **Fig. 1** Daily (a) and cumulative (b) biogas yield of co-digestion systems with the  
557 addition of  $\text{Fe}_2\text{O}_3$  and  $n\text{Fe}_2\text{O}_3$ .

558 **Fig. 2** The stability performances of co-digestion systems with the addition of  $\text{Fe}_2\text{O}_3$   
559 and  $n\text{Fe}_2\text{O}_3$ .

560 Fig. 2a: pH; Fig. 2b: IA/PA; Fig. 2c: TAN; Fig. 2d: COD (Chemical oxygen demand)

561 **Fig. 3** Daily (a) and cumulative (b) biogas yield of co-digestion systems with the  
562 addition of  $\text{Fe}_3\text{O}_4$  and  $n\text{Fe}_3\text{O}_4$ .

563 **Fig. 4** The stability performances of co-digestion systems with different additives.

564 Fig. 4a: pH; Fig. 4b: IA/PA; Fig. 4c: TAN; Fig. 4d: COD

565 **Fig. 5** The estimated by kinetic model for the cumulative biogas yield with different  
566 additives.

567 Fig. 5a:  $\text{Fe}_2\text{O}_3$  ; Fig. 5b:  $n\text{Fe}_2\text{O}_3$ ,; Fig. 5c:  $\text{Fe}_3\text{O}_4$ ; Fig. 5d:  $n\text{Fe}_3\text{O}_4$

568 **Fig. 6** The correlation analysis of AD factors.

569 **Fig. 7** The possible causes of promotion and inhibition at different conditions.

570

571

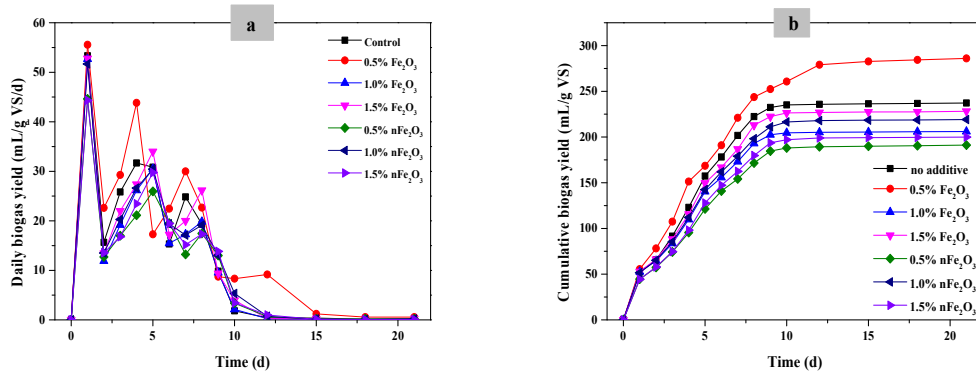
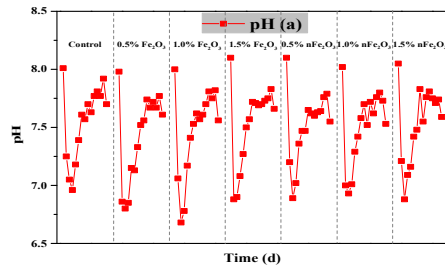
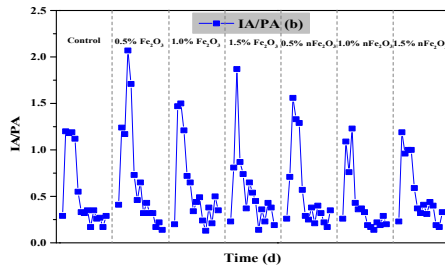


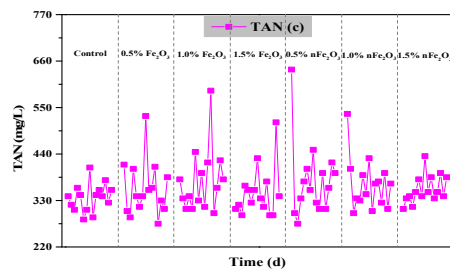
**Fig. 1.** Daily (a) and cumulative (b) biogas yield of co-digestion systems with the addition of Fe<sub>2</sub>O<sub>3</sub> and nFe<sub>2</sub>O<sub>3</sub>.



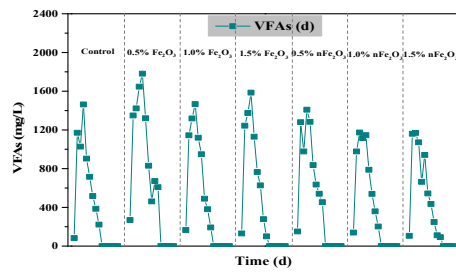
573



574



575

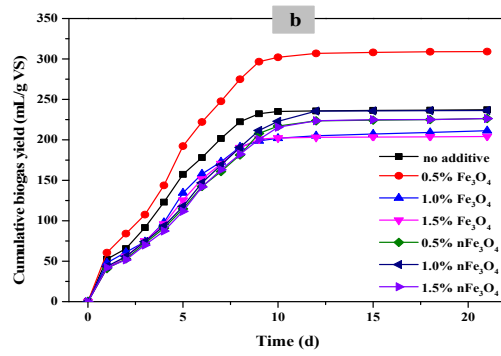
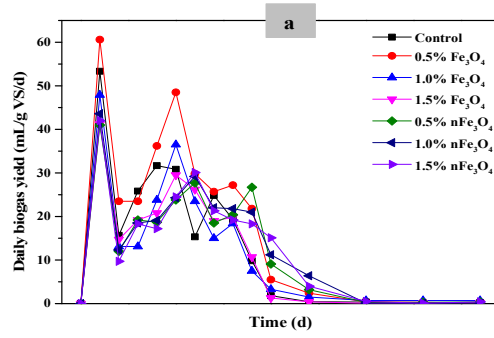


576

577 **Fig. 2.** The stability performances of co-digestion systems with the addition of  $\text{Fe}_2\text{O}_3$  and  $\text{nFe}_2\text{O}_3$ :

578 (a) pH; (b) IA/PA; (c) TAN; and (d) COD (Chemical oxygen demand).

579



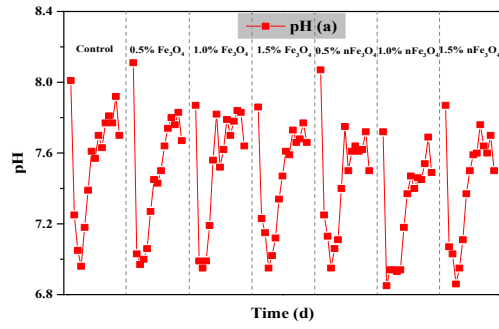
580

581

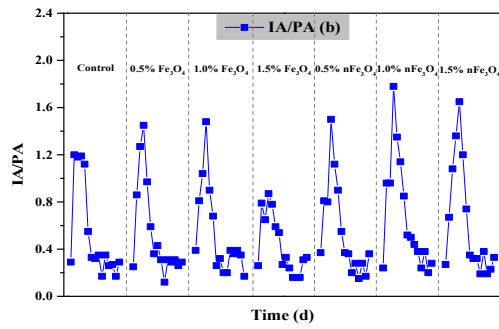
582 **Fig. 3.** Daily (a) and cumulative (b) biogas yield of co-digestion systems with the addition of

583

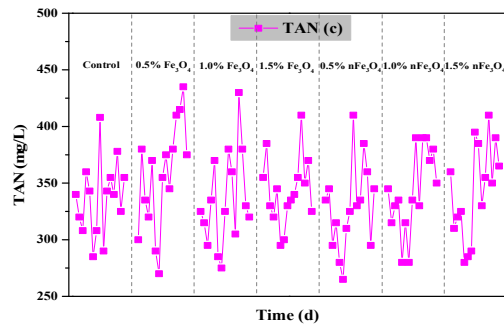
$\text{Fe}_3\text{O}_4$  and  $\text{nFe}_3\text{O}_4$ .



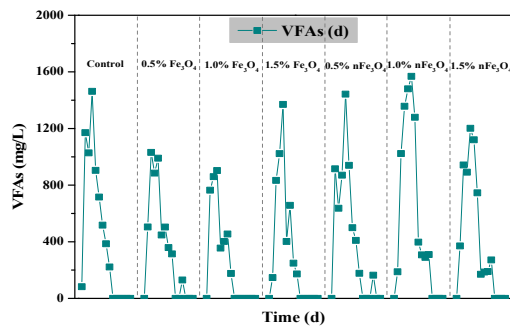
584



585



586

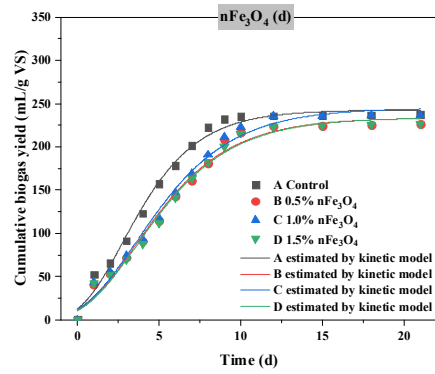
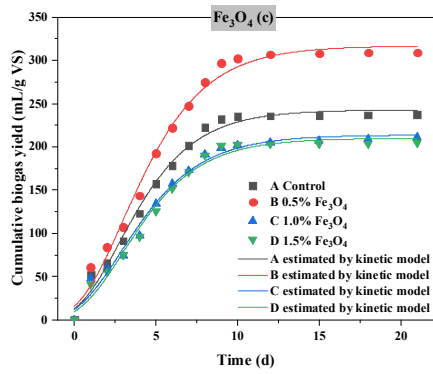
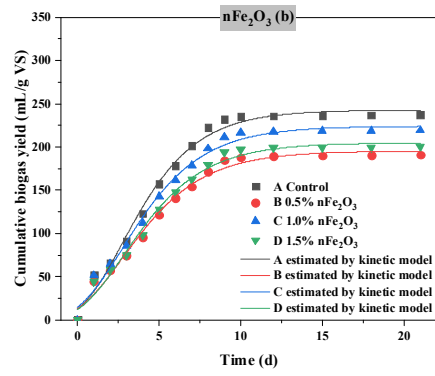
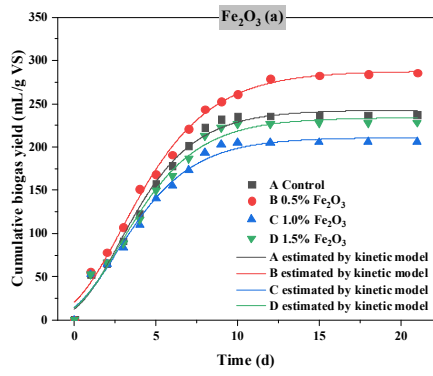


587

588

Fig. 4. The stability performances of co-digestion systems with different additives.

589



590

591

592

**Fig. 5.** The estimated by kinetic model for the cumulative biogas yield with different additives.

593

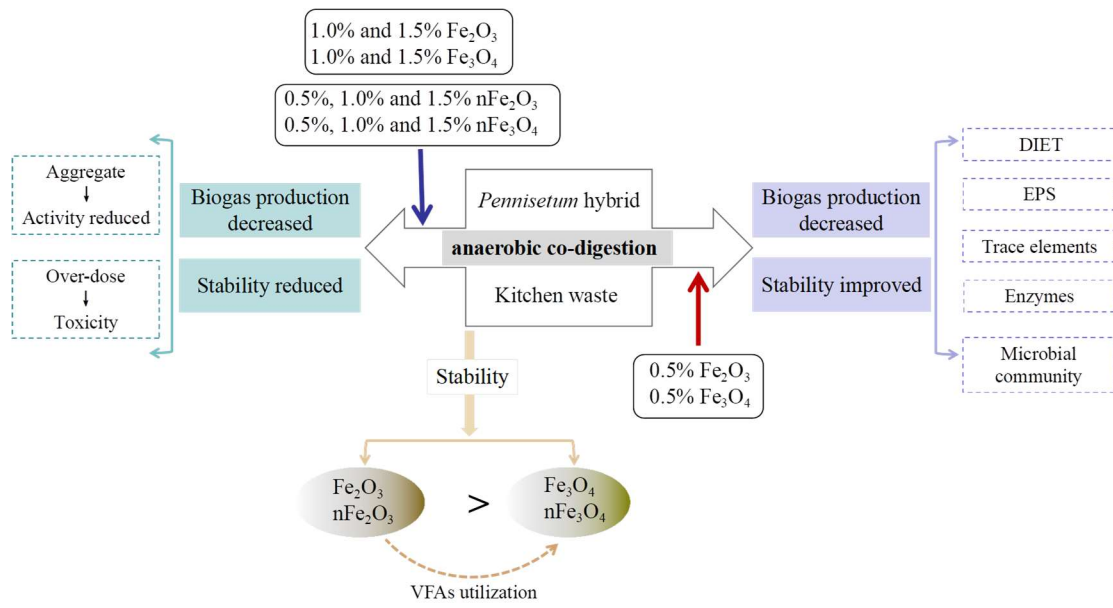
		$r_s$			
		pH	IA/PA	TAN	VFAs
Cumulative biogas yield	Control	+0.540*	-0.698**	+0.308	-0.824**
	0.5% Fe <sub>2</sub> O <sub>3</sub>	+0.529*	-0.821**	-0.039	-0.771**
	1.0% Fe <sub>2</sub> O <sub>3</sub>	+0.500	-0.439	+0.279	-0.821**
	1.5% Fe <sub>2</sub> O <sub>3</sub>	+0.493	-0.559*	+0.179	-0.850**
	0.5% nFe <sub>2</sub> O <sub>3</sub>	+0.474	-0.561*	+0.161	-0.806**
	1.0% nFe <sub>2</sub> O <sub>3</sub>	+0.479	-0.679**	-0.191	-0.810**
	1.5% nFe <sub>2</sub> O <sub>3</sub>	+0.386	-0.563*	+0.551*	-0.822**
	0.5% Fe <sub>3</sub> O <sub>4</sub>	+0.571*	-0.551*	+0.624*	-0.664*
	1.0% Fe <sub>3</sub> O <sub>4</sub>	+0.461	-0.644*	+0.331	0.688*
	1.5% Fe <sub>3</sub> O <sub>4</sub>	+0.524*	-0.603*	+0.138	-0.599*
	0.5% nFe <sub>3</sub> O <sub>4</sub>	+0.390	-0.768**	+0.329	-0.622*
	1.0% nFe <sub>3</sub> O <sub>4</sub>	+0.570*	-0.616*	+0.595*	-0.484
	1.5% nFe <sub>3</sub> O <sub>4</sub>	+0.476	-0.553*	+0.554*	-0.589*

594

595

**Fig. 6.** Correlation analysis of AD factors.

596



597

598

**Fig. 7.** The possible causes of promotion and inhibition at different conditions.

599



600

601

